Tumor and Stem Cell Biology

Cancer Research

The Bisecting GlcNAc on *N*-Glycans Inhibits Growth Factor Signaling and Retards Mammary Tumor Progression

Yinghui Song[1], Jason A. Aglipay[1], Joshua D. Bernstein[2], Sumanta Goswami[2], and Pamela Stanley[1]

Abstract

The branching of complex *N*-glycans attached to growth factor receptors promotes tumor progression by prolonging growth factor signaling. The addition of the bisecting GlcNAc to complex *N*-glycans by Mgat3 has varying effects on cell adhesion, cell migration, and hepatoma formation. Here, we show that Chinese hamster ovary cells expressing Mgat3 and the polyoma middle T (PyMT) antigen have reduced cell proliferation and growth factor signaling dependent on a galectin lattice. The *Mgat3* gene is not expressed in virgin mammary gland but is upregulated during lactation and is expressed in mouse mammary tumor virus (MMTV)/PyMT tumors. Mice lacking Mgat3 that cannot transfer the bisecting GlcNAc to *N*-glycans acquire PyMT-induced mammary tumors more rapidly and have an increased tumor burden, increased migration of tumor cells, and increased early metastasis to lung. Tumors and tumor-derived cells lacking Mgat3 exhibit enhanced signaling through the Ras pathway and reduced amounts of functionally glycosylated α-dystroglycan. Constitutive overexpression of an MMTV/*Mgat3* transgene inhibits early mammary tumor development and tumor cell migration. Thus, the addition of the bisecting GlcNAc to complex *N*-glycans of mammary tumor cell glycoprotein receptors is a cell autonomous mechanism serving to retard tumor progression by reducing growth factor signaling. *Cancer Res; 70(8); 3361–71. ©2010 AACR.*

Introduction

N-glycans have a common core structure, and their branching patterns are determined by different *N*-acetylglucosaminyltransferases (GlcNAcT; ref. 1). Loss of GlcNAcT-V (Mgat5), an *N*-acetylglucosaminyltransferase that initiates a β1,6 branch of complex *N*-glycans, promotes tumorigenesis in the mammary glands of mice carrying the mouse mammary tumor virus (MMTV) polyoma middle T (PyMT) oncogene (2). Mammary tumor cells expressing Mgat5 are more responsive to growth factors due to enhanced interactions of their growth factor receptors with galectins, leading to reduced endocytosis and prolonged signaling compared with cells lacking Mgat5 (3, 4). Human cancer cell lines with targeted silencing of the *Mgat5* gene also exhibit reduced epidermal growth factor (EGF) receptor (EGFR) signaling, although apparently by a galectin-independent mechanism (5).

Mgat3 transfers a GlcNAc to generate the bisecting GlcNAc in the core of complex and hybrid *N*-glycans (ref. 6; Fig. 1A). The presence of the bisecting GlcNAc alters glycan recognition reflected by changes in the binding of plant lectins and mammalian galectins. Thus, LEC10 Chinese hamster ovary (CHO) cells that express Mgat3 (7, 8) bind markedly less ricin and more erythrophytohemagglutinin (E-PHA) than wild-type CHO cells (Fig. 1A). LEC10 cells also bind less galectin-1 and galectin-3 than parent CHO cells (9). These lectin-binding properties reflect changes in the number or accessibility of Gal residues on cell surface *N*-glycans with a bisecting GlcNAc. Glycomics profiling of LEC10 *N*-glycans by matrix-assisted laser desorption/ionization–time-of-flight mass spectrometry shows that the bisecting GlcNAc is present on complex, multiantennary *N*-glycans with many LacNAc units (10).

Mgat3 has been overexpressed in a broad spectrum of cells with consequences that may vary with cell type (11, 12). Thus, overexpression of Mgat3 in K562 cells causes an increase in spleen colonization (13), whereas overexpression in B16 melanoma cells causes a marked reduction in homing to the lung (14). In HeLa cells, overexpresion of Mgat3 causes increased EGFR signaling and reduced cell adhesion, promoting metastasis (15). However in other experiments, HeLa cells overexpressing Mgat3 had reduced cell migration on fibronectin, countering metastasis (16). When Mgat3 was overexpressed in MKN45 cells, E-cadherin was upregulated, cell adhesion was enhanced, and cell migration was inhibited (12, 17). The combined data indicate that Mgat3 may behave as a promoter or suppressor of cell migration and cell adhesion. In liver tumors induced by a low dose of diethylnitrosamine, ~50% of males expressing Mgat3 under the serum amyloid protein promoter got fewer tumors (18). By contrast, Mgat3 expressed under the mouse urinary protein promoter was not inhibitory (19) when diethylnitrosamine

Authors' Affiliations: [1]Department of Cell Biology, Albert Einstein College of Medicine of Yeshiva University, Bronx, New York and [2]Department of Biology, Yeshiva University, New York, New York

Note: Supplementary data for this article are available at Cancer Research Online (http://cancerres.aacrjournals.org/).

Corresponding Author: Pamela Stanley, Department of Cell Biology, Albert Einstein College of Medicine, 1300 Morris Park Avenue, Bronx, NY 10461. Phone: 718-430-3346; Fax: 718-430-8574; E-mail: pamela.stanley@einstein.yu.edu.

doi: 10.1158/0008-5472.CAN-09-2719

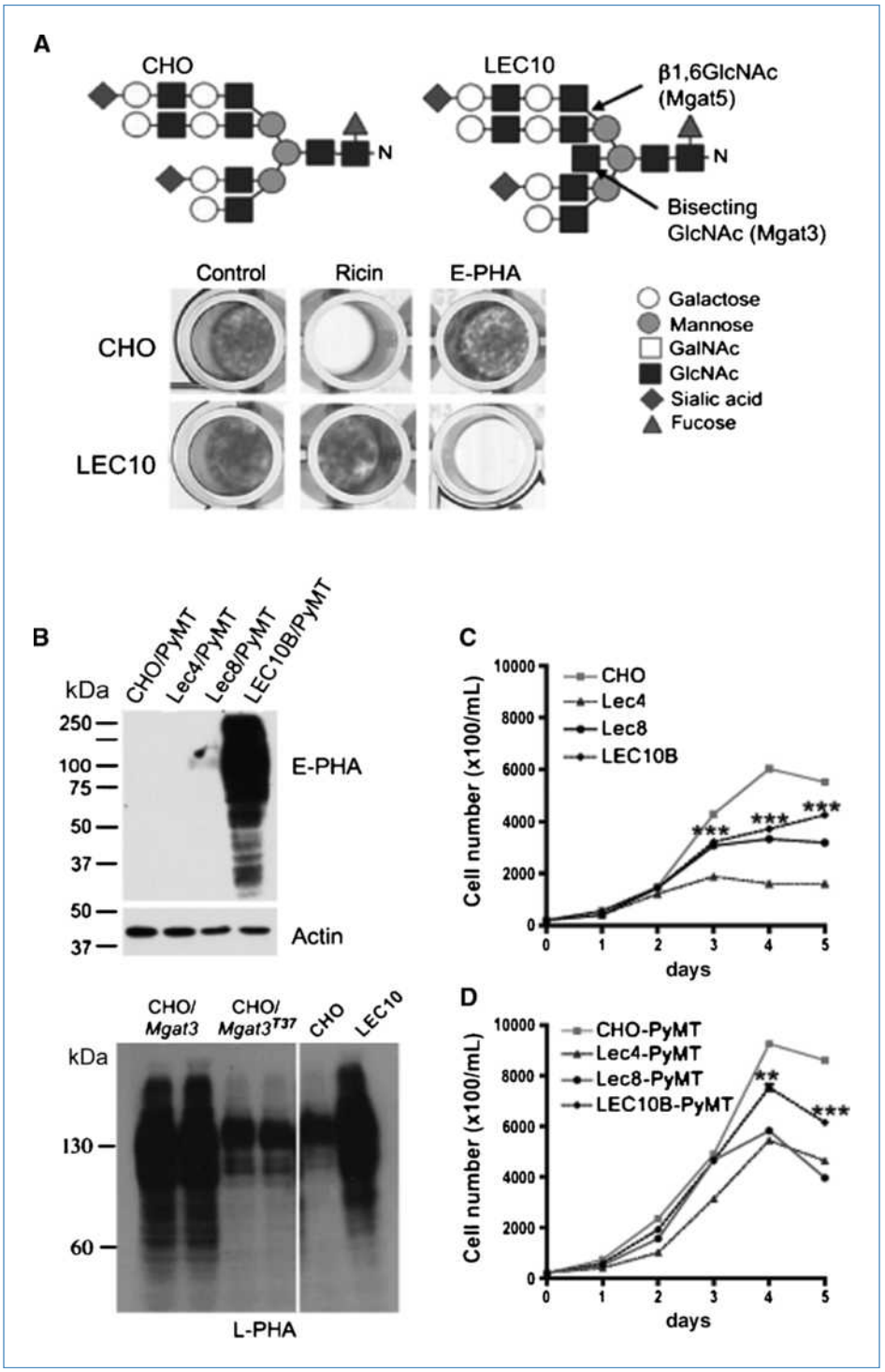

Figure 1. Mgat3 retards cell proliferation. A, complex *N*-glycans of CHO and LEC10 showing the reactions catalyzed by Mgat3 and Mgat5 (top). LEC10 cells are resistant to ricin and hypersensitive to E-PHA (bottom). B, glycoproteins expressing the bisecting GlcNAc bind well to biotinylated E-PHA (top) and biotinylated L-PHA (bottom). C, proliferation of CHO, Lec4, Lec8, and LEC10 in medium with 7.5% serum. D, proliferation of CHO/PyMT, Lec4/PyMT, Lec8/PyMT, and LEC10B/PyMT in medium with 7.5% serum. Bars, SD. ***, $P < 0.0001$; **, $P < 0.01$, two-tailed Student's *t* test comparing CHO with LEC10B.

and phenobarbitol were used. In addition, males with independent, targeted mutations of the *Mgat3* gene developed hepatomas more slowly than controls (19, 20), consistent with the facilitation of hepatoma progression by Mgat3.

We report here the effects of Mgat3 and the bisecting GlcNAc on growth factor signaling in CHO cells expressing PyMT and in the mammary gland during tumor induction by MMTV/PyMT (21). The MMTV/PyMT female develops tumors at different rates in all mammary glands, depending on genetic background (22). Progression to malignancy in this model appropriately reflects the stages of human breast tumorigenesis (23). The PyMT oncoprotein activates signaling

pathways commonly amplified in human breast cancer, such as phosphoinositide 3-kinase, leading to activation of Akt, Ras-Raf, and mitogen-activated protein kinases (MAPK; ref. 24). Here we show that Mgat3 inhibits growth factor signaling dependent on a cell surface galectin lattice in CHO cells and functions cell autonomously in the mammary gland to retard tumor progression, cell migration, and metastasis in MMTV/PyMT-induced tumors.

Materials and Methods

Cells and cell culture. Pro$^-$5 CHO, Lec4 (Pro$^-$Lec4.7B), Lec8 (Pro$^-$Lec8.3D), and LEC10B (Pro$^-$LEC10B.3) cells (25) validated by lectin resistance test and used within 6 mo of cloning were transfected with pcDNA3.1-PyMT generated from PJΩ-PyVMT (Elaine Lin; Albert Einstein College Medicine) and selected with 1 mg/mL G418 (Invitrogen). CHO and LEC10 cells were transfected with the *Mgat3* coding exon or inactive Mgat3 (*Mgat3*^{T37}; ref. 26) in pcDNA3.1. CHO cells were cultured in α$^+$-MEM (Invitrogen) containing 10% fetal bovine serum (FBS) and 2 mmol/L glutamine at 37°C in 5% CO_2. Tumor epithelial cells (TEC) were derived from minced tumors treated with 2 mg/mL collagenase (Sigma) and passaged ~22 times to selectively remove fibroblasts. TECs were cultured in α$^+$-MEM containing 10% heat-inactivated FBS, penicillin, and streptomycin.

Lectin resistance test. Cells (2×10^3) at 100 μL/well in a 96-well plate were incubated with 100 μL medium or medium with ricin (5 ng/mL; Vector Labs) or E-PHA (35 μg/mL; Vector Labs) for 4 d, stained with methylene blue in 50% methanol (2 g/L), and photographed.

Western blot analysis and lectin blotting. Frozen tumor (~150 mg) homogenized in 1 mL 10 mmol/L Tris-HCl (pH 7.4), 0.25 mol/L sucrose, and protease inhibitors (Complete; Roche) was centrifuged at 1,800 rpm for 10 min at 4°C. Tumor cells or washed cultured cells were solubilized in 2% Triton-X-100, incubated on ice for 10 min, and centrifuged at 3,000 rpm for 10 min at 4°C. Protein concentration was measured using the DC reagent (Bio-Rad). Lysates in loading buffer containing β-mercaptoethanol (5%) were heated at 95°C for 5 min and separated by 12% SDS-PAGE. Proteins were transferred to a Polyscreen polyvinylidene difluoride (PVDF) membrane (PerkinElmer) in Tris-glycine buffer containing 5% methanol. For Western blot analysis, membranes were incubated in 5% nonfat milk and primary antibody at room temperature for 1 h. Mouse anti-β-actin monoclonal antibody (mAb; Abcam AC-15; 1:5,000), mouse anti-α-dystroglycan (α-DG) mAb IIH6C4 (Upstate Biotechnology-Millipore; 1:1,000), mouse anti-β-DG mAb (43DAG1/8DG; Novocastra Laboratories; 1:300), horseradish peroxidase (HRP)–conjugated goat anti-mouse IgG (H+L; Thermo Scientific; 1:10,000), HRP goat anti-rabbit IgG-H+L (Zymed; 1:10,000). After three washes with TBS-Tween [10 mmol/L Tris-HCl (pH 7.4), 150 mmol/L NaCl, 0.05% Tween 20 (Sigma)], secondary antibody HRP was incubated for 1 h. Bands were visualized using an enhanced chemiluminescence (ECL) kit (Thermo Scientific) and quantitated by NIH Image/J. For lectin blotting, membranes were blocked in 5% nonfat milk, incubated with biotinylated E-PHA or leukophytohemagglutinin (L-PHA; Vector Labs) at 5 μg/mL at room temperature for 1 h, washed with TBS-Tween, incubated with streptavadin-HRP (1:5,000; Vector Labs) for 1 h, and visualized using an ECL kit.

Signaling assays. Cells (85% to 90% confluent in 60-mm dishes) were serum-starved for 24 h. After washing with α$^+$-MEM, cells were stimulated with 10% FCS, 50 ng/mL human platelet-derived growth factor-AB (PDGF-AB; Invitrogen), or 50 ng/mL EGF (R&D Systems) at 37°C. For sugar treatments after starvation, 1.5 mL α$^+$-MEM or 0.5 mol/L lactose or 0.5 mol/L sucrose in α$^+$-MEM was added for 1 h at 37°C, cells were washed twice with α$^+$-MEM and treated with FCS, EGF, or PDGF-AB at 37°C. MAPK/extracellular signal-regulated kinase kinase 1/2 (MEK1/2) inhibitor UO126 (Cell Signaling) was dissolved in DMSO at 10 mmol/L, added at ≤10 μmol/L for 2 h, and removed before adding growth factor. Controls were treated with DMSO. After stimulation, cells were washed thrice with PBS (pH 7.4), lysed in EBC lysis buffer [50 mmol/L Tris-HCl (pH 8.0), 120 mmol/L NaCl, 0.5% NP40, 100 mmol/L NaF, 200 μmol/L sodium orthovanadate] containing protease inhibitors (Complete, Roche), electrophoresed and transferred to PVDF membrane. Membranes were incubated with rabbit anti-phosphorylated p44/42 MAPK antibody (Thr^{202}/Tyr^{204}; 1:1,000) and mouse anti-p44/42 MAPK mAb (L34F12; 1:2,000; Cell Signaling Technology) in Odyssey blocking buffer at 4°C overnight. Following washes with TBS-Tween, IRDye800-conjugated goat anti-rabbit IgG-H+L (MX10, Rockland Immunochemicals; 1:10,000), Alexa Fluor^{680} goat anti-mouse IgG-H+L (Invitrogen; 1:15,000) were added for 1 h at room temperature, membranes were washed, and bands were quantitated by ODYSSEY IR Imaging System (LI-COR BioSciences).

Mice. *Mgat3*$^{-/-}$ mice (*Mgat3*^{tm1Jxm}; ref. 27) backcrossed to C57Bl/6 mice were mated with MMTV/PyMT transgenic mice (634 FVB; ref. 21; Jeffrey Pollard; Albert Einstein College of Medicine). *Mgat3*$^{+/-}$ or *Mgat3*$^{-/-}$ females and *Mgat3*$^{+/-}$ MMTV/PyMT males were mated to generate *Mgat3*$^{+/+}$/PyMT, *Mgat3*$^{+/-}$/PyMT, and *Mgat3*$^{-/-}$/PyMT littermates. The C57Bl/6/FVB background slowed the time of onset and progression of mammary tumors (22, 28).

The MMTV-SV40-BssK vector (Jeffrey Pollard) was used to make the MMTV-*Mgat3*-CAG*loxP*CAT*loxP*-EGFP transgene. The mouse *Mgat3* coding region was inserted between the MMTV-LTR and the SV40-polyA addition site followed by the CAG*loxP*CAT*loxP*-EGFP cassette (ref. 29; Jun-ichi Miyazaki; Osaka University Medical School). Plasmid linearized by *Spe*1 was microinjected into FVB fertilized eggs. A founder with a single site of integration and several tandem copies of the *Mgat3* transgene was used to generate MMTV-*Mgat3*-PyMT mice. Mice were housed in a barrier facility with food and water *ad libitum*. Animal protocols were approved by the Animal Institute Committee of the Albert Einstein College of Medicine.

Tumor analysis. All 10 mammary glands of MMTV/PyMT females were palpated (genotype-blinded) thrice a week, from 6 wk. The three largest mammary tumors were excised, weighed, and fixed in 10% formalin at room temperature for

24 h. Tumor tissue was also frozen in Trizol (Invitrogen) or stored at −80°C. Total RNA from tumors was analyzed by reverse transcription–PCR (RT-PCR) to determine expression of PyMT, Mgat3, Mgat5, and β-actin (primers in Supplementary Table S1).

Lung metastasis. Formalin-fixed lungs were paraffin-embedded and sectioned at 5 μm. Three sections per lung separated by 50 μm were stained with H&E and examined for metastatic lesions. Total RNA extracted from lungs in Trizol (Invitrogen) was treated with amplification grade DNaseI (Invitrogen) and cDNA prepared using the SuperScript III first-strand synthesis system (Invitrogen). Real-time PCR was performed with 5 ng cDNA and primers: PyMT, 5′-agccactcctatcccccaac-3′ (forward), 5′-ctcctcctcctcctcctcca-3′ (reverse); β-actin, 5′-gtgggccgctctaggcacca-3′ (forward), 5′-tggccttagggttcaggggg-3′ (reverse). PCR products incorporated SYBR Green dye (Qiagen) and were analyzed on a Prism 7700 system (Applied Biosystems) as follows: 95°C 15 min, then 94°C 15 s, 59°C 30 s, 72°C 30 s for 40 cycles. PCR product formation was measured continuously, and C(t) plots were generated. Plasmids TA-PyMT and TA-actin were used to determine the absolute number of PyMT and mouse β-actin transcripts.

In vivo *invasion assay.* Cell migration into microneedles filled with 25 nmol/L EGF (Invitrogen) and Matrigel (BD Biosciences) and placed into tumors of live anesthetized animals was performed as described (30). Passive collection of cells or tissue during insertion of needles was blocked. After 4 h, needles were removed and cell numbers were determined by 4′,6-diamidino-2-phenylindole staining. Cell migration is required for cells to enter needles (31).

Statistical analysis. Student's *t* test was from the Excel Data Analysis Package. Tumor development was compared by Mantel-Cox log-rank test. Univariate analysis was performed by the χ^2 test.

Results

Mgat3 inhibits growth factor signaling in CHO/PyMT cells. To investigate effects of the bisecting GlcNAc and PyMT on growth factor signaling, we used PyMT-expressing CHO mutants whose glycosylation pathways are extremely well characterized (10, 25). Wild-type CHO cells lack Mgat3 but express Mgat5, LEC10B express Mgat3 and Mgat5, Lec4 lack both Mgat3 and Mgat5, and galectin binding is CHO>LEC10B∼Lec4 (9). Lec8 lacks Gal residues on all glycans and does not bind galectins (9). As expected, glycoproteins with the bisecting GlcNAc from LEC10B/PyMT bound E-PHA and those without did not (Fig. 1B). However, glycoproteins from LEC10 or CHO Mgat3 transfectants also bound L-PHA highly compared with cells expressing inactive Mgat3^{T37} (Fig. 1B). Therefore Mgat3 does not interfere with Mgat5 in CHO cells.

The effect of the bisecting GlcNAc on growth rate was determined in medium with reduced FBS. All CHO cells expressing PyMT grew at a faster rate (Fig. 1C and D). At 7.5% FBS LEC10B/PyMT with the bisecting GlcNAc on complex *N*-glycans proliferated more slowly than CHO/PyMT. Lec4 with reduced *N*-glycan branching and Lec8 lacking Gal grew slower than CHO and LEC10B, whether they were expressing PyMT or not (Fig. 1C and D).

Activation of the Ras pathway was also investigated. After serum starvation for 24 h, cells were stimulated by 50 ng/mL PDGF-AB. All cells expressed similar cell surface levels of the PDGF receptor (PDGFR; Supplementary Fig. S1). The ratio of pErk-1/2/Erk-1/2 was greatest after 5 minutes in all cells (Fig. 2A). This ratio was reduced by ∼40% to 50% in LEC10B/PyMT and Lec4/PyMT and to an even greater extent in Lec8/PyMT cells that lack Gal on glycans (Fig. 2B). Similar results were obtained for 10% serum. Treatment with the MEK kinase inhibitor UO126 inhibited both Erk-1/2 activation and cell proliferation (Supplementary Fig. S2).

The responses of PyMT transfectants to growth factors correlated with their reduced ability to bind galectin-1 and galectin-3 (CHO>LEC10B∼Lec4≫Lec8; ref. 9). Consistent with a role for galectins, PDGF-induced Erk-1 activation was strongly inhibited by treatment with lactose, which removes galectins from the CHO cell surface (9), whereas sucrose had no effect (Fig. 2C and D). The same results were obtained for Erk-2. Thus, galectins enhance signaling via PDGFRs that carry wild-type complex *N*-glycans to a greater extent than PDGFRs with bisected complex *N*-glycans (LEC10B) or complex *N*-glycans lacking a β1,6 branch (Lec4) or lacking Gal residues (Lec8).

Mgat3 is expressed in lactating mammary glands and PyMT tumors. RT-PCR on total RNA from the fourth mammary gland failed to detect *Mgat3* expression in virgins but showed robust expression during lactation (Fig. 3A). Reflecting active Mgat3, glycoproteins from lactating mammary glands bound E-PHA much better than those from non-lactating mammary glands (Fig. 3B). In mammary tumors, the *PyMT* oncogene was expressed equivalently in control (*Mgat3*$^{+/-}$/PyMT) and mutant (*Mgat3*$^{-/-}$/PyMT) females (Fig. 3C). *Mgat3* transcripts, although undetected in virgin mammary glands, were present in mammary tumors of *Mgat3*$^{+/-}$/PyMT virgins (Fig. 3C). Mgat5 transcripts were also not detected in virgin mammary glands but were present in mammary tumors, irrespective of *Mgat3* genotype (Fig. 3C). Glycoproteins from *Mgat3*$^{+/-}$/PyMT tumors bound E-PHA better than those from *Mgat3*$^{-/-}$/PyMT tumors or virgin mammary glands (Fig. 3D). *Mgat3* gene expression did not affect the expression of *Mgat5* (Fig. 3C) nor L-PHA binding to tumor glycoproteins.

The absence of Mgat3 enhances tumor development. Mammary tumor development in *Mgat3*$^{+/+}$/PyMT (n = 4) and *Mgat3*$^{+/-}$/PyMT (n = 23) females was shown to be equivalent (days to first tumor, 74 ± 1.7 versus 75 ± 2.3; days to first five tumors, 90.5 ± 3.4 versus 91.6 ± 2.22; weight of largest three tumors, 1.3 ± 0.2 g versus 1.2 ± 0.2 g, respectively, based on mean ± SEM), allowing *Mgat3*$^{+/-}$/PyMT females to serve as controls. Early tumor lesions were examined by whole-mount analysis of the fourth mammary gland. Expression of Mgat3 correlated with a reduced primary tumor lesion in several 5-week littermate pairs (Supplementary Fig. S3). The average lesion area was 3.2 mm^2 in 5-week *Mgat3*$^{+/-}$/PyMT females (n = 8) compared with 4.5 mm^2 in mutant

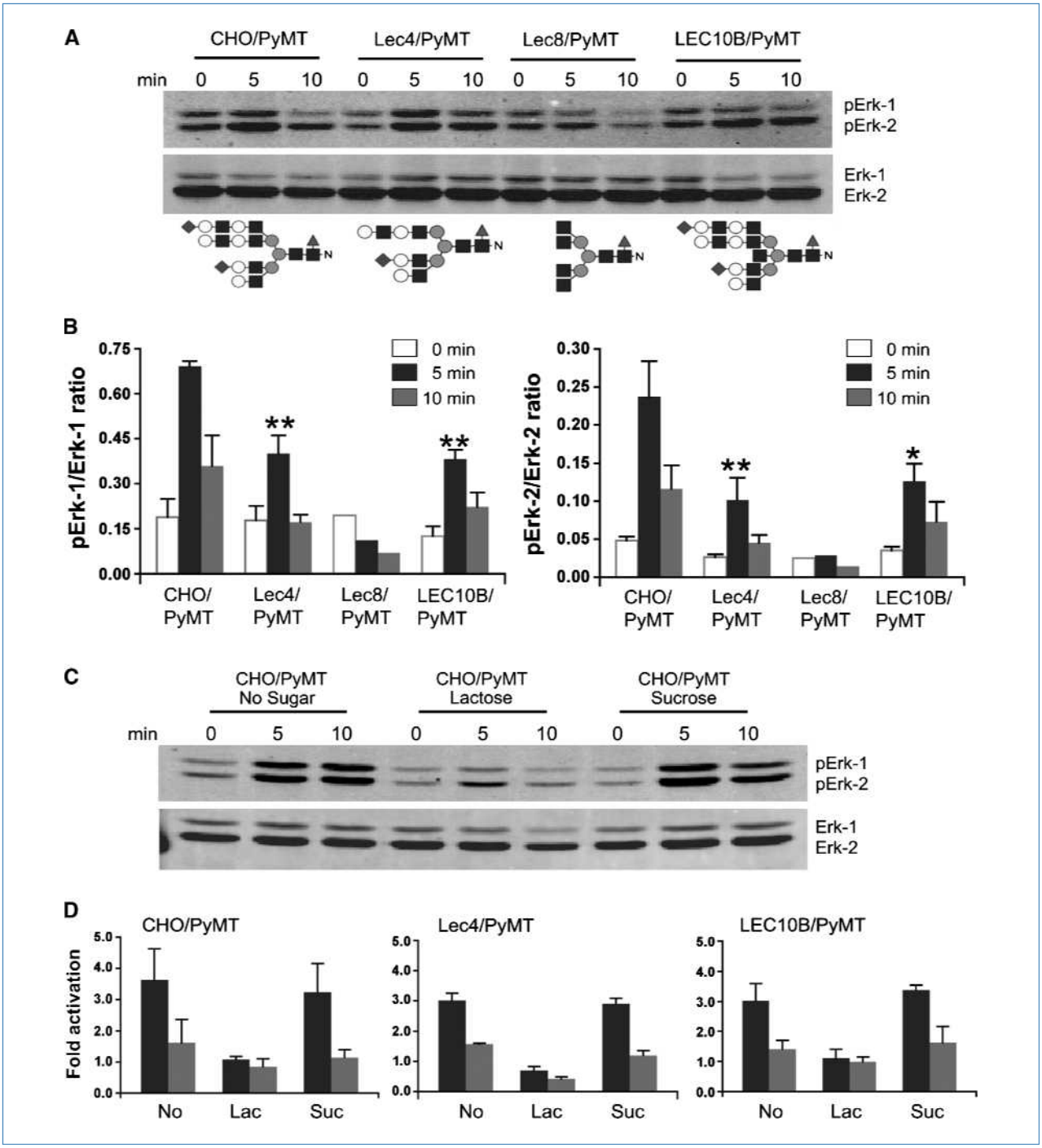

Figure 2. Galectin-regulated PDGF signaling is reduced by Mgat3. A, Western blot of pErk-1/2 and Erk-1/2 in PyMT CHO cells. The *N*-glycans are typical of the cell line. Symbols in Fig. 1A. B, ratios of pErk-1/Erk-1 and pErk-2/Erk-2 after 50 ng/mL PDGF-AB ($n = 5$). Bars, SEM. **, $P < 0.001$, two-tailed Student's *t* test; *, $P < 0.05$, one-tailed Student's *t* test comparing CHO to Lec4 or LEC10B. C, Western blot of pErk-1/2 and Erk-1/2 in CHO/PyMT cells after treatment with 0.5 mol/L lactose or sucrose. D, effects of lactose on PDGF signaling. Fold activation of pErk1/Erk1 at 5 and 10 min compared with 0 min after 50 ng/mL PDGF ($n = 3$). Bars, SEM.

females ($n = 9$), but significance was $P > 0.05$. At 5 weeks all mammary tumors were adenomas.

Tumor development was examined by palpation from 6 weeks. *Mgat3*$^{-/-}$/PyMT mutants had a palpable tumor ~7 days earlier than controls, and they were also ~8 days ahead in having five palpable mammary tumors (Fig. 4A). Analysis of tumor development in all 10 mammary glands shows that control females remained tumor-free for a

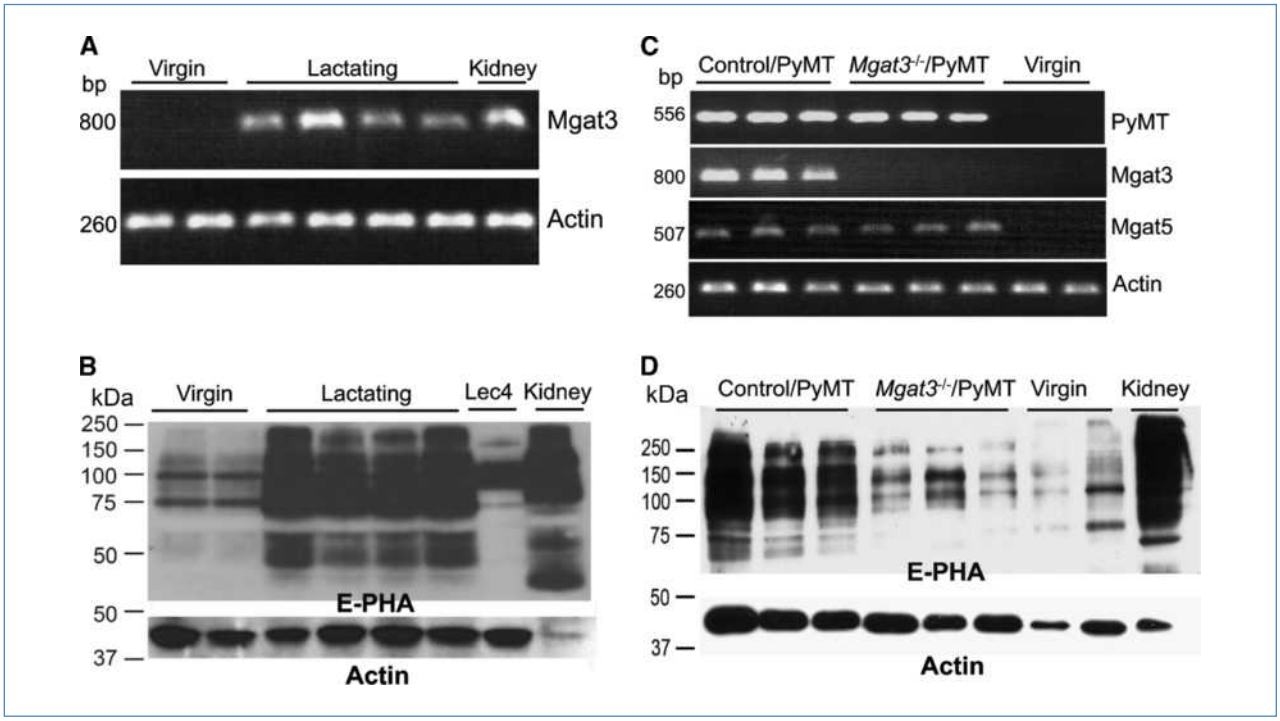

Figure 3. *Mgat3* is expressed in lactating mammary gland and MMTV/PyMT tumors. A, RT-PCR of total RNA from the fourth mammary gland of 4-month virgin or lactating females. B, glycoproteins (~80 μg) from lactating mammary gland of the same females bound E-PHA. Lec4 glycoproteins lack and kidney glycoproteins (~5 μg) carry the bisecting GlcNAc. C, representative RT-PCR of total RNA from tumors of $Mgat3^{+/-}$/PyMT(n = 13) and $Mgat3^{-/-}$/PyMT(n = 7) females at 17 wks. D, glycoproteins (~80 μg) with the bisecting GlcNAc bound E-PHA.

significantly longer time than mice lacking Mgat3 (Fig. 4B). At 17 weeks, 17 of 20 $Mgat3^{-/-}$/PyMT females had tumors in all 10 mammary glands compared with only 9 of 23 $Mgat3^{+/-}$/PyMT control mice.

Tumor burden is increased in the absence of Mgat3. The largest three tumors from 17-week mice were weighed. The absence of Mgat3 substantially affected tumor burden, increasing it by ~1.7-fold (Fig. 4C). Among the 60 tumors from mutant mice, ~30% weighed >1 g, whereas from control mice only ~10% weighed >1 g (Fig. 4D). Body weight was similar for control and mutant females at 17 weeks.

Erk-1/2 phosphorylation is increased in* Mgat3$^{-/-}$*/PyMT mammary tumors and TECs. Erk-1/2 activation was analyzed in tumor tissue and compared by the ratios pErk-1/2/Erk-1/2. Tumors from 17-week $Mgat3^{-/-}$/PyMT females exhibited greater levels of Erk-1/2 activation compared with controls (Fig. 5A). This was also found in tumors from 15-week females. Similarly, TECs derived from $Mgat3^{-/-}$/PyMT tumors exhibited greater Erk-1/2 activation than $Mgat3^{+/-}$/PyMT TECs following EGF or PDGF-AB stimulation (Fig. 5B). Independent TEC lines gave similar results with serum or EGF stimulation (Supplementary Fig. S4). Both signaling and proliferation of TECs were inhibited by UO126 (Fig. 5B; Supplementary Fig. S5). Thus, the increased tumor progression of $Mgat3^{-/-}$/PyMT tumors seems to be due in part to increased signaling via the Ras pathway, consistent with results from LEC10B/PyMT cells (Fig. 2) showing that the bisecting GlcNAc on *N*-glycans of GFRs reduces growth factor signaling.

Loss of Mgat3 causes increased pulmonary metastases. Western blot analyses showed that $Mgat3^{-/-}$/PyMT tumors from three 15-week females expressed low amounts of functionally glycosylated α-DG recognized by mAb IIH6 (Fig. 5C), indicating enhanced metastatic potential (32, 33). This loss of IIH6 reactivity was confirmed in two $Mgat3^{-/-}$/PyMT TEC lines (Fig. 5C). Lung metastases in control and mutant females were assayed by real-time PCR of PyMT transcripts in lung (34, 35). Total RNA was isolated from whole lungs of 8-week mice when mammary tumors were at the adenoma or early carcinoma stage. The absolute copy number of PyMT and β-actin was determined and the PyMT/actin ratio calculated. There was more PyMT expression in lungs of females lacking Mgat3 (Fig. 5D). This was also apparent in a plot of PyMT/actin transcript ratio compared with tumor lesion area (Fig. 5D). In mammary glands with the least tumor size, $Mgat3^{-/-}$/PyMT lungs generated more PyMT transcripts than controls, in which the number of PyMT transcripts was relatively constant in relation to tumor area. By contrast, lung PyMT transcripts generally increased with tumor area in $Mgat3^{-/-}$/PyMT mammary glands. Therefore, the absence of Mgat3 facilitates early lung metastasis from $Mgat3^{-/-}$/PyMT tumors. By 17 weeks however, mutant and control lungs had many metastases in equivalent numbers based on histologic comparisons of lung sections.

Constitutive overexpression of Mgat3 retards early tumor formation. Because virgin mammary glands do not express Mgat3 (Fig. 3) and $Mgat3^{+/+}$/PyMT virgins do not

begin to express Mgat3 until ~4 to 5 weeks, the effect of constitutively misexpressing Mgat3 under the MMTV promoter was investigated. Expression of the MMTV-*Mgat3* transgene was confirmed by RT-PCR (Fig. 6A), and Mgat3 activity was shown by lectin blotting with E-PHA (Fig. 6B). Nontransgenic 5-week mammary tumor glycoproteins did not bind E-PHA. Tumor lesions in whole mounts of the fourth mammary gland were reduced in MMTV-*Mgat3*-PyMT transgenic females (Fig. 6C). Therefore constitutive overexpression of the *Mgat3* gene inhibited the development of primary tumors at 4.5 weeks. However, a comparison at 13 weeks when PyMT tumors express Mgat3 revealed no significant difference in the tumor burden of MMTV-Mgat3-PyMT and control females.

Tumor cell migration is inhibited by Mgat3. A hallmark of enhanced progression of tumors is the acquisition of migratory properties by tumor cells (31). To investigate the effect of Mgat3 on tumor cell migration, cells that migrated into needles containing EGF and inserted into tumors were counted. In tumors lacking Mgat3, cell migration into both control and EGF-containing needles was increased (Fig. 6D). In tumors from Mgat3 overexpressing females, cell migration into both control and EGF-containing needles was reduced (Fig. 6D). Therefore Mgat3 inhibits the acquisition of migratory properties by mammary tumor cells.

Discussion

Understanding factors that affect tumor progression is important for determining how to control tumor growth and metastasis. Here we show that the addition of a single bisecting GlcNAc by Mgat3 to complex *N*-glycans on GFRs has pronounced effects on tumor progression. In the MMTV/PyMT mammary gland, premature expression of Mgat3 inhibits the development of primary tumor lesions and tumor cell migration. Conversely, when the *Mgat3* gene is inactivated, mammary tumors appear earlier, develop more rapidly, contain more migratory tumor cells, and metastasize earlier to lung. The *Mgat3* gene is not expressed in virgin mammary gland but is upregulated during MMTV/PyMT tumorigenesis. Mgat3 is similarly upregulated in WAP/SV40 T antigen (36) and MMTV/neu (37) mouse mammary tumors. The modification of E-cadherin by Mgat3 reduces its turnover and enhances cell-cell interactions (38, 39). Therefore, Mgat3 upregulation during tumor formation may be part of a cellular attempt to suppress tumor progression. We observed no evidence of spontaneous mammary tumor formation in C57Bl/6 *Mgat3*$^{-/-}$ females following five cycles of pregnancy and lactation, although C57Bl/6 mice are relatively resistant to mammary tumor development (22, 28). In humans, the *MGAT3* gene maps to 22q13.1, in a

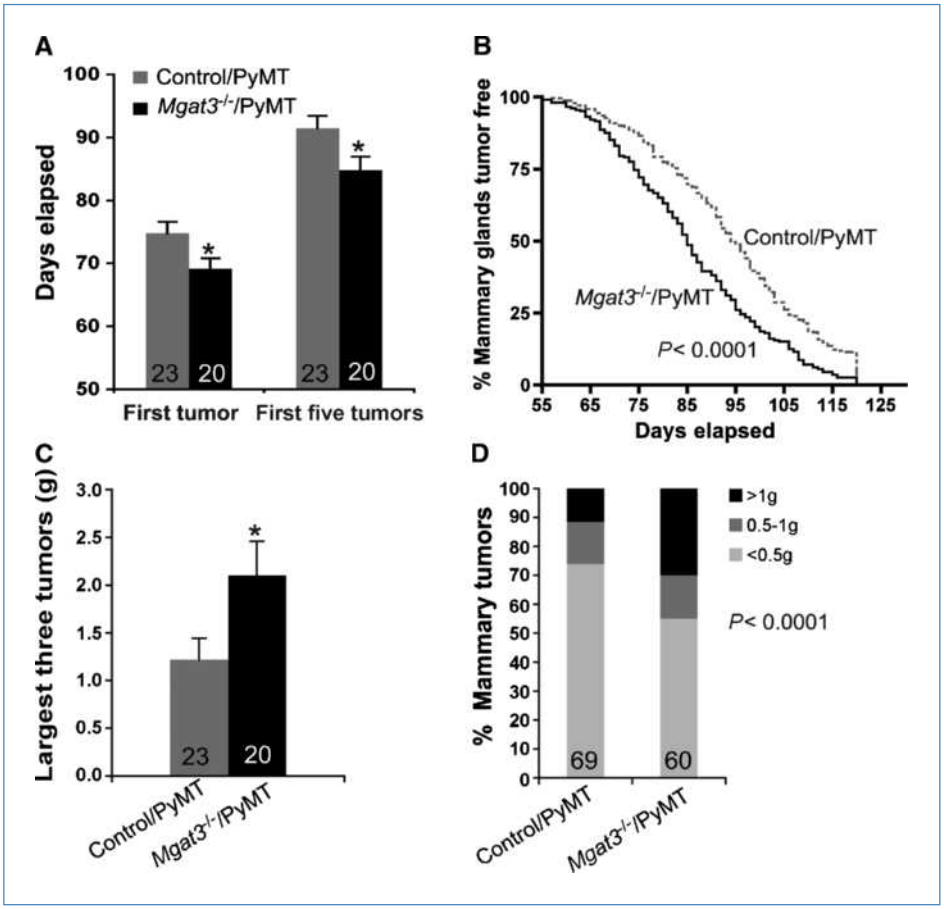

Figure 4. Tumor burden is increased in the absence of Mgat3. A, *Mgat3*$^{+/-}$/PyMT (Control) and *Mgat3*$^{-/-}$/PyMT mammary glands were palpated beginning at week 6. Times to first and first five palpable tumors. *, $P < 0.05$, two-tailed Student's *t* test. Bars, SEM. B, percentage of *Mgat3*$^{+/-}$/PyMT (Control) and *Mgat3*$^{-/-}$/PyMT mammary glands tumor free to 17 wks (Kaplan-Meier plot; ***, $P < 0.0001$, Mantel-Cox log-rank test). C, weight of the largest three tumors from *Mgat3*$^{+/-}$/PyMT (Control) and *Mgat3*$^{-/-}$/PyMT females at 17 wks. *, $P < 0.05$, two-tailed Student's *t* test. Bars, SEM. D, weight of each tumor from *Mgat3*$^{-/-}$/PyMT ($n = 60$) and control ($n = 69$) females. ***, $P < 0.0001$, χ^2 test.

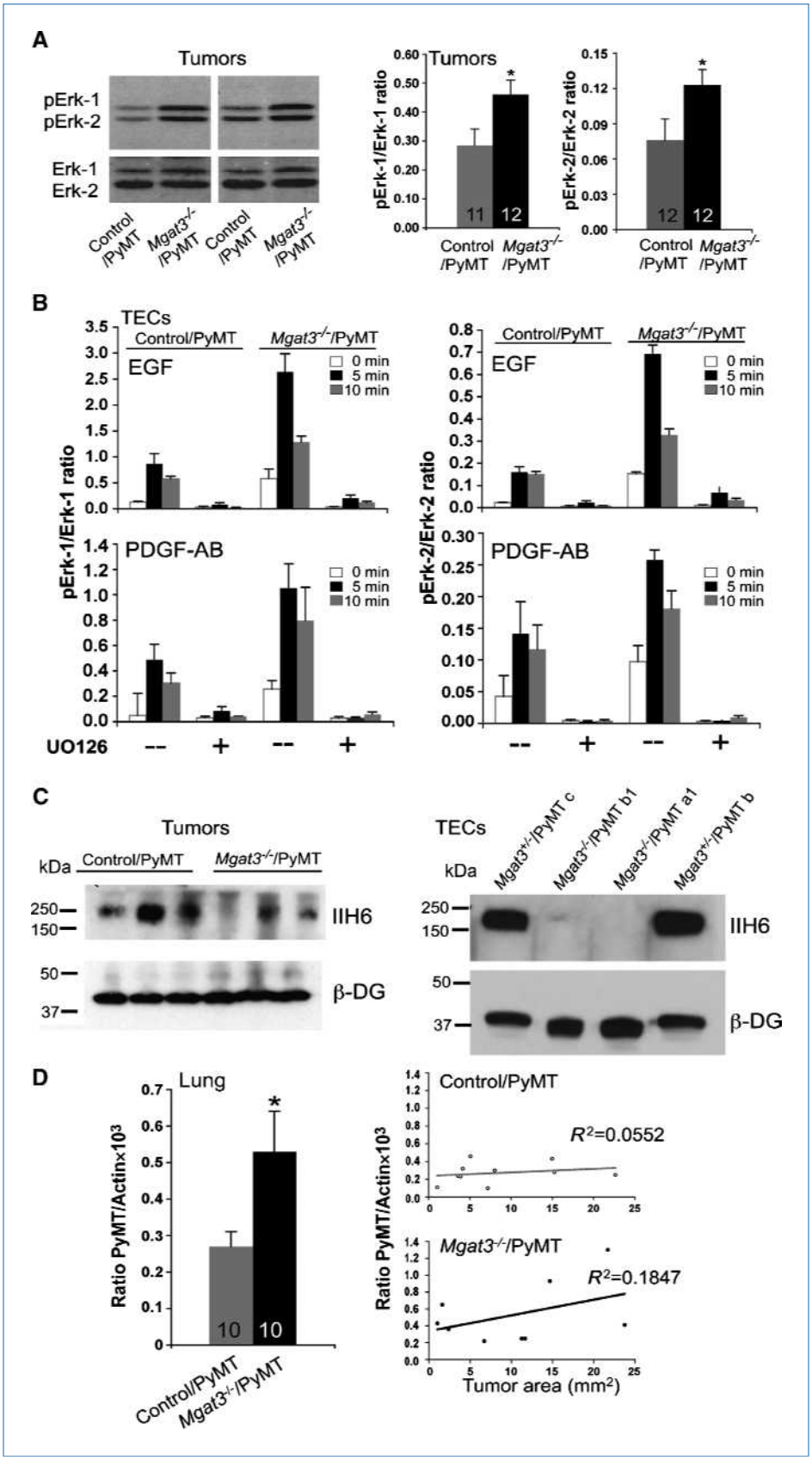

Figure 5. Increased expression of pErk-1/2 and early pulmonary metastases in the absence of Mgat3. A, Western blot of pErk-1/2 and Erk-1/2 in tumors from *Mgat3*$^{+/-}$/PyMT and *Mgat3*$^{-/-}$/PyMT females. Ratios of pErk-1/Erk-1 and pErk-2/Erk-2 in histograms. *, $P < 0.05$, two-tailed Student's *t* test. Bars, SEM. B, EGF and PDGF-AB signaling in *Mgat3*$^{+/-}$/PyMT and *Mgat3*$^{-/-}$/PyMT TECs in the presence and absence of 10 μmol/L UO126. Bars, SEM. C, functionally glycosylated α-DG (IIH6) in 15-wk tumors and TEC lines. D, ratio absolute number PyMT/actin (×10^3) transcripts. *, $P < 0.05$, two-tailed Student's *t* test. Bars, SEM (left). Ratio absolute number PyMT/actin (×10^3) transcripts versus tumor area from the fourth mammary gland of the same mice (right).

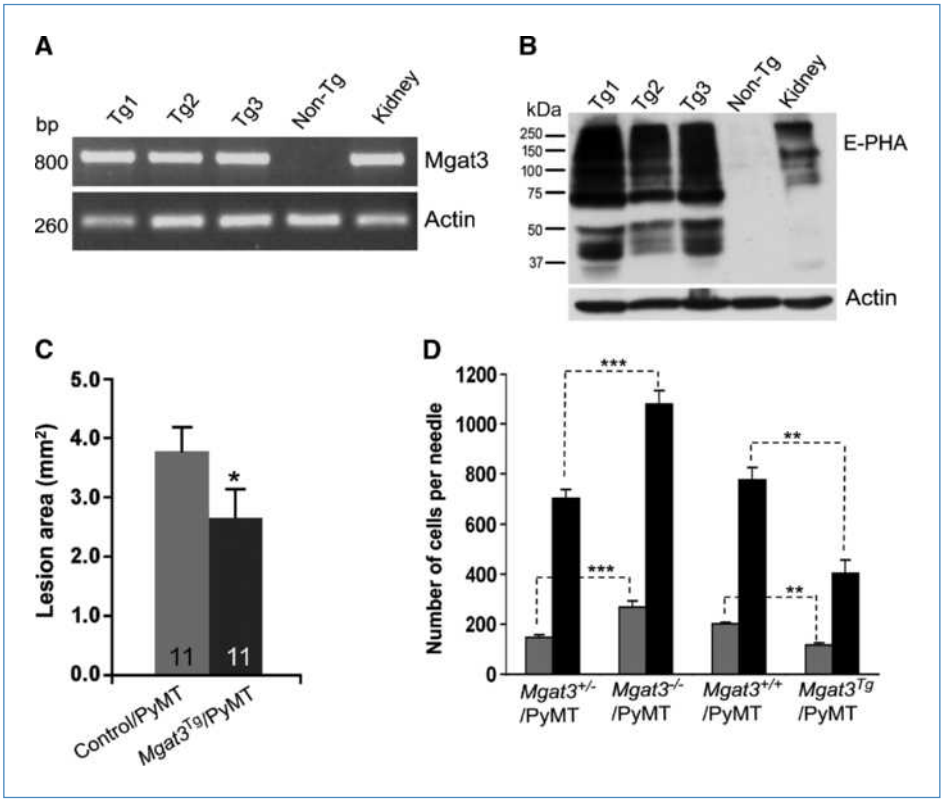

Figure 6. Constitutive overexpression of Mgat3 inhibits early mammary tumor development. A, RT-PCR of total RNA from the fourth mammary gland of 5-wk virgin transgenic (Tg) or non-transgenic females; kidney cDNA, positive control. B, glycoproteins with bisected *N*-glycans from the other mammary gland of the same females bound E-PHA. C, tumor lesion areas in control and MMTV-*Mgat3*-PyMT transgenic mice. *, $P < 0.05$, one-tailed Student's *t* test. Bars, SEM. D, cells collected in control ($n = 2$) or EGF-containing needles ($n = 4$) inserted for 4 h into mammary tumors ($n = 4$–6) of ~1.5 cm.

region proposed to contain a tumor suppressor gene whose loss of heterozygosity (LOH) correlates with human breast cancers (40, 41). Expression data from human breast cancers have not revealed changes in Mgat3 transcripts to date, perhaps because *MGAT3* mutations do not alter the expression of mutant alleles maintained by LOH. In human ovarian cancer, however, upregulation of the *MGAT3* gene was observed (42).

To address how the loss of Mgat3 might promote tumor progression, we examined growth factor signaling in CHO/PyMT cells, MMTV/PyMT tumors, and MMTV/PyMT TEC cells. In LEC10B CHO cells with well-characterized bisected *N*-glycans (10) that cause a reduction in cell surface galectin binding (9), Mgat3 expression retards cell proliferation and inhibits galectin-promoted growth factor signaling. Importantly, CHO/PyMT cell proliferation is driven in part by Erk-1/2 activation as shown by the inhibition of cell growth by the MEK1/2 inhibitor UO126. Erk-1/2 activation is also regulated by Mgat3 *in vivo*, being greater in *Mgat3*$^{-/-}$/PyMT mammary tumors. Tumor-derived TECs lacking Mgat3 also exhibited enhanced Erk-1/2 activation in response to serum, EGF, or PDGF. Therefore, whereas the MMTV/PyMT oncogene was the driving force of mammary tumorigenesis, Mgat3 restrained growth factor signaling, and loss of Mgat3 resulted in an increase in Erk-1/2 activation.

PyMT is a scaffold protein that acts in the cytoplasm to cause transformation (24). It cannot be directly affected by Mgat3, which acts on *N*-glycans in the Golgi. This is the reason our investigations into how Mgat3 modulates mammary tumor progression focused on its effects on growth factor signaling via glycoprotein receptors such as PDGFR and EGFR known to have *N*-glycans modified by Mgat3 (15). Constitutive activation of EGF signaling due to activating mutations in EGFRs is a well-characterized basis of poor prognosis in breast cancer (43). PDGF signaling has also been implicated in both autocrine and paracrine mechanisms of promoting breast cancer progression (44, 45). A new mechanism for modulating signaling through GFRs is through interactions of lactosamine units on their complex *N*-glycans via a galectin lattice (46, 47). GFRs with more branched *N*-glycans are retained longer at the cell surface in a galectin lattice, allowing them to signal longer before endocytosis and downregulation. This is the mechanism that we propose is affected by the addition of the bisecting GlcNAc. Thus, we show that loss of Mgat3 reduces galectin-regulated growth factor signaling and cell proliferation. Growth factor receptors with a bisecting GlcNAc are predicted to be less well retained in a galectin lattice and to signal more weakly than their counterparts with *N*-glycans lacking the bisecting GlcNAc. We propose that reduced galectin lattice interactions caused by the bisecting GcNAc are due to reduced galectin recognition of highly branched *N*-glycans carrying a bisecting GlcNAc. An alternative proposal that bisected complex *N*-glycans are not substrates for Mgat5 and thereby have reduced branching (13) seems unlikely because LEC10 glycoproteins carrying the bisecting GlcNAc bind much more L-PHA (which recognizes the product of Mgat5) than CHO glycoproteins and express *N*-glycans with many LacNAc

units (10), indicating that branched N-glyans are likely to have been produced by Mgat5.

Any growth factor or cytokine receptor or integrin with complex *N*-glycans is a potential substrate for Mgat3 and may have its signaling strength modulated by the addition of the bisecting GlcNAc. Thus, a broad spectrum of signaling pathways may be affected in MMTV/PyMT tumor cells. In this paper, we focus on Erk-1/2 activation and show a functional relationship to cell proliferation. It will be important in the future to determine the hierarchy of growth-promoting versus growth-retarding pathways, as well as those involved in epithelial-mesenchymal transition and metastasis that are modulated by Mgat3 during MMTV/PyMT tumor progression. For example, we observed that 15-week mammary tumors and TECs lacking Mgat3 express reduced levels of functionally glycosylated α-DG, which results in reduced binding to laminin and correlates with enhanced tumor progression (32, 33). Loss of another GlcNAcT (β1,3GlcNAcT-1), which is essential to the generation of lactosamine units on complex *N*-glycans and also to the functional glycosylation of α-DG, also leads to enhanced progression in a murine prostate cancer model (32). Mgat3 transfers the bisecting GlcNAc to the same subset of complex *N*-glycans that are substrates for β1,3GlcNAcT-1 and may act, in part, by inhibiting the functional glycosylation of *N*-glycans on α-DG, which are known substrates of Large (48), a putative glycosyltransferase for which β1,3GlcNAcT-1 is an essential partner (32).

In investigations of mechanism, it will also be important to identify which of the 10 mouse galectins promote the progression of MMTV/PyMT mammary tumors through their interactions with complex *N*-glycans. Whereas galectin-3 has been implicated in the regulation of growth factor signaling in MMTV/PyMT tumors (3), females lacking galectin-3 generate equivalent numbers of MMTV/PyMT mammary tumors to controls (49). In addition, galectin-3 is downregulated and poorly expressed during lactation in the mouse (50). Therefore, one or more of the other mouse galectins seem to be important for tumor progression in the murine mammary gland.

In conclusion, it is apparent that addition of the bisecting GlcNAc to complex *N*-glycans on mammary glycoproteins serves to protect mammary epithelial cells from tumor progression. Thus, loss of Mgat3 by LOH in human cancers would be expected to promote tumor progression.

Disclosure of Potential Conflicts of Interest

No potential conflicts of interest were disclosed.

Acknowledgments

We thank Elaine Lin and Jeffrey Pollard for expert advice; Riddhi Battarycharrya, Peter Draber, David Gross, Yan Deng, and Wen Dong for technical assistance; Shira Landskorner-Eiger, Suzannah Williams, and Paraic Kenny for helpful discussions; and all who kindly provided reagents.

Grant Support

National Cancer Institute grants RO130645 and RO136434 (P. Stanley) and P30CA013330 supporting the Albert Einstein Cancer Center and Young Investigator Award Breast Cancer Alliance, Inc. (S. Goswami).

The costs of publication of this article were defrayed in part by the payment of page charges. This article must therefore be hereby marked *advertisement* in accordance with 18 U.S.C. Section 1734 solely to indicate this fact.

Received 07/22/2009; revised 01/05/2010; accepted 01/22/2010.

References

1. Stanley P, Schachter H, Taniguchi N. In: Varki A, Cummings RD, Esko JD, Freeze HH, Stanley P, Bertozzi CR, Hart GW, Etzler ME, editors. *N*-glycans. Essentials of gycobiology. 2nd ed Cold Spring Harbor: Cold Spring Harbor Laboratory Press; 2009, p. 101–14.
2. Granovsky M, Fata J, Pawling J, Muller WJ, Khokha R, Dennis JW. Suppression of tumor growth and metastasis in Mgat5-deficient mice. Nat Med 2000;6:306–12.
3. Partridge EA, Le Roy C, Di Guglielmo GM, et al. Regulation of cytokine receptors by Golgi *N*-glycan processing and endocytosis. Science 2004;306:120–4.
4. Lau K, Partridge E, Grigorian A, et al. Complex *N*-glycan number and degree of branching cooperate to regulate cell proliferation and differentiation. Cell 2007;129:123–34.
5. Guo HB, Johnson H, Randolph M, Lee I, Pierce M. Knockdown of GnT-Va expression inhibits ligand-induced downregulation of the epidermal growth factor receptor and intracellular signaling by inhibiting receptor endocytosis. Glycobiology 2009;19:547–59.
6. Narasimhan S. Control of glycoprotein synthesis. UDP-GlcNAc: glycopeptide β 4-N-acetylglucosaminyltransferase III, an enzyme in hen oviduct which adds GlcNAc in β 1–4 linkage to the β-linked mannose of the trimannosyl core of N-glycosyl oligosaccharides. J Biol Chem 1982;257:10235–42.
7. Campbell C, Stanley P. A dominant mutation to ricin resistance in Chinese hamster ovary cells induces UDP-GlcNAc:glycopeptide β-4-N-acetylglucosaminyltransferase III activity. J Biol Chem 1984; 259:13370–8.
8. Stanley P, Sundaram S, Tang J, Shi S. Molecular analysis of three gain-of-function CHO mutants that add the bisecting GlcNAc to *N*-glycans. Glycobiology 2005;15:43–53.
9. Patnaik SK, Potvin B, Carlsson S, Sturm D, Leffler H, Stanley P. Complex *N*-glycans are the major ligands for galectin-1, -3, and -8 on Chinese hamster ovary cells. Glycobiology 2006;16:305–17.
10. North SJ, Huang H-H, Sundaram S, et al. Glycomics profiling of Chinese hamster ovary (CHO) cell glycosylation mutants reveals *N*-glycans of a novel size and complexity. J Biol Chem 2010;285: 5759–75.
11. Zhao Y, Sato Y, Isaji T, et al. Branched *N*-glycans regulate the biological functions of integrins and cadherins. FEBS J 2008;275:1939–48.
12. Takahashi M, Kuroki Y, Ohtsubo K, Taniguchi N. Core fucose and bisecting GlcNAc, the direct modifiers of the *N*-glycan core: their functions and target proteins. Carbohydr Res 2009;344:1387–90.
13. Yoshimura M, Ihara Y, Ohnishi A, et al. Bisecting N-acetylglucosamine on K562 cells suppresses natural killer cytotoxicity and promotes spleen colonization. Cancer Res 1996;56:412–8.
14. Yoshimura M, Nishikawa A, Ihara Y, Taniguchi S, Taniguchi N. Suppression of lung metastasis of B16 mouse melanoma by N-acetylglucosaminyltransferase III gene transfection. Proc Natl Acad Sci U S A 1995;92:8754–8.
15. Sato Y, Takahashi M, Shibukawa Y, et al. Overexpression of N-acetylglucosaminyltransferase III enhances the epidermal growth factor-induced phosphorylation of ERK in HeLaS3 cells by up-regulation of the internalization rate of the receptors. J Biol Chem 2001;276:11956–62.
16. Isaji T, Gu J, Nishiuchi R, et al. Introduction of bisecting GlcNAc into

integrin α5β1 reduces ligand binding and down-regulates cell adhesion and cell migration. J Biol Chem 2004;279:19747–54.
17. Akama R, Sato Y, Kariya Y, et al. N-acetylglucosaminyltransferase III expression is regulated by cell-cell adhesion via the E-cadherin-catenin-actin complex. Proteomics 2008;8:3221–8.
18. Ekuni A, Miyoshi E, Ko JH, et al. A glycomic approach to hepatic tumors in N-acetylglucosaminyltransferase III (GnT-III) transgenic mice induced by diethylnitrosamine (DEN): identification of haptoglobin as a target molecule of GnT-III. Free Radic Res 2002;36:827–33.
19. Yang X, Bhaumik M, Bhattacharyya R, Gong S, Rogler CE, Stanley P. New evidence for an extra-hepatic role of N-acetylglucosaminyltransferase III in the progression of diethylnitrosamine-induced liver tumors in mice. Cancer Res 2000;60:3313–9.
20. Yang X, Tang J, Rogler CE, Stanley P. Reduced hepatocyte proliferation is the basis of retarded liver tumor progression and liver regeneration in mice lacking N-acetylglucosaminyltransferase III. Cancer Res 2003;63:7753–9.
21. Guy CT, Cardiff RD, Muller WJ. Induction of mammary tumors by expression of polyomavirus middle T oncogene: a transgenic mouse model for metastatic disease. Mol Cell Biol 1992;12:954–61.
22. Qiu TH, Chandramouli GV, Hunter KW, Alkharouf NW, Green JE, Liu ET. Global expression profiling identifies signatures of tumor virulence in MMTV/PyMT-transgenic mice: correlation to human disease. Cancer Res 2004;64:5973–81.
23. Lin EY, Jones JG, Li P, et al. Progression to malignancy in the polyoma middle T oncoprotein mouse breast cancer model provides a reliable model for human diseases. Am J Pathol 2003;163:2113–26.
24. Dilworth SM. Polyoma virus middle T antigen and its role in identifying cancer-related molecules. Nat Rev Cancer 2002;2:951–6.
25. Patnaik SK, Stanley P. Lectin-resistant CHO glycosylation mutants. Methods Enzymol 2006;416:159–82.
26. Bhattacharyya R, Bhaumik M, Raju TS, Stanley P. Truncated, inactive N-acetylglucosaminyltransferase III (GlcNAc-TIII) induces neurological and other traits absent in mice that lack GlcNAc-TIII. J Biol Chem 2002;277:26300–9.
27. Priatel JJ, Sarkar M, Schachter H, Marth JD. Isolation, characterization and inactivation of the mouse Mgat3 gene: the bisecting N-acetylglucosamine in asparagine-linked oligosaccharides appears dispensable for viability and reproduction. Glycobiology 1997;7:45–56.
28. Davie SA, Maglione JE, Manner CK, et al. Effects of FVB/NJ and C57Bl/6J strain backgrounds on mammary tumor phenotype in inducible nitric oxide synthase deficient mice. Transgenic Res 2007;16:193–201.
29. Kawamoto S, Niwa H, Tashiro F, et al. A novel reporter mouse strain that expresses enhanced green fluorescent protein upon Cre-mediated recombination. FEBS Lett 2000;470:263–8.
30. Wyckoff JB, Segall JE, Condeelis JS. The collection of the motile population of cells from a living tumor. Cancer Res 2000;60:5401–4.
31. Wyckoff J, Wang W, Lin EY, et al. A paracrine loop between tumor cells and macrophages is required for tumor cell migration in mammary tumors. Cancer Res 2004;64:7022–9.
32. Bao X, Kobayashi M, Hatakeyama S, et al. Tumor suppressor function of laminin-binding α-dystroglycan requires a distinct β3-N-acetylglucosaminyltransferase. Proc Natl Acad Sci U S A 2009;106:12109–14.
33. de Bernabé DB, Inamori K, Yoshida-Moriguchi T, et al. Loss of α-dystroglycan laminin binding in epithelium-derived cancers is caused by silencing of LARGE. J Biol Chem 2009;284:11279–84.
34. Montagna C, Lyu MS, Hunter K, et al. The Septin 9 (MSF) gene is amplified and overexpressed in mouse mammary gland adenocarcinomas and human breast cancer cell lines. Cancer Res 2003;63:2179–87.
35. Zheng H, Abdel Aziz HO, Nakanishi Y, et al. Oncogenic role of JC virus in lung cancer. J Pathol 2007;212:306–15.
36. Klein A, Guhl E, Zollinger R, et al. Gene expression profiling: cell cycle deregulation and aneuploidy do not cause breast cancer formation in WAP-SVT/t transgenic animals. J Mol Med 2005;83:362–76.
37. Landis MD, Seachrist DD, Montanez-Wiscovich ME, Danielpour D, Keri RA. Gene expression profiling of cancer progression reveals intrinsic regulation of transforming growth factor-β signaling in ErbB2/Neu-induced tumors from transgenic mice. Oncogene 2005;24:5173–90.
38. Iijima J, Zhao Y, Isaji T, et al. Cell-cell interaction-dependent regulation of N-acetylglucosaminyltransferase III and the bisected *N*-glycans in GE11 epithelial cells. Involvement of E-cadherin-mediated cell adhesion. J Biol Chem 2006;281:13038–46.
39. Yoshimura M, Ihara Y, Matsuzawa Y, Taniguchi N. Aberrant glycosylation of E-cadherin enhances cell-cell binding to suppress metastasis. J Biol Chem 1996;271:13811–5.
40. Iida A, Kurose K, Isobe R, et al. Mapping of a new target region of allelic loss to a 2-cM interval at 22q13.1 in primary breast cancer. Genes Chromosomes Cancer 1998;21:108–12.
41. Nagahata T, Hirano A, Utada Y, et al. Correlation of allelic losses and clinicopathological factors in 504 primary breast cancers. Breast Cancer 2002;9:208–15.
42. Abbott KL, Nairn AV, Hall EM, et al. Focused glycomic analysis of the N-linked glycan biosynthetic pathway in ovarian cancer. Proteomics 2008;8:3210–20.
43. Hynes NE, MacDonald G. ErbB receptors and signaling pathways in cancer. Curr Opin Cell Biol 2009;21:177–84.
44. Jechlinger M, Sommer A, Moriggl R, et al. Autocrine PDGFR signaling promotes mammary cancer metastasis. J Clin Invest 2006;116:1561–70.
45. Roussidis AE, Theocharis AD, Tzanakakis GN, Karamanos NK. The importance of c-Kit and PDGF receptors as potential targets for molecular therapy in breast cancer. Curr Med Chem 2007;14:735–43.
46. Dennis JW, Lau KS, Demetriou M, Nabi IR. Adaptive regulation at the cell surface by N-glycosylation. Traffic 2009;10:1569–78.
47. Lajoie P, Goetz JG, Dennis JW, Nabi IR. Lattices, rafts, and scaffolds: domain regulation of receptor signaling at the plasma membrane. J Cell Biol 2009;185:381–5.
48. Patnaik SK, Stanley P. Mouse large can modify complex N- and mucin O-glycans on α-dystroglycan to induce laminin binding. J Biol Chem 2005;280:20851–9.
49. Eude-Le Parco I, Gendronneau G, Dang T, et al. Genetic assessment of the importance of galectin-3 in cancer initiation, progression, and dissemination in mice. Glycobiology 2009;19:68–75.
50. Ron M, Israeli G, Seroussi E, et al. Combining mouse mammary gland gene expression and comparative mapping for the identification of candidate genes for QTL of milk production traits in cattle. BMC Genomics 2007;8:183.